NIPPON STEEL TECHNICAL REPORT No. 103 MAY 2013

Technical Report

UDC 620 . 162

Evaluation and Improving Methods of Stretch Flangeability

Hiroshi YOSHIDA*
Koichi SATO
Takashi MATSUNO
Tohru YOSHIDA
Yuzo TAKAHASHI
Jun NITTA

Abstract

By using of high strength steel sheets for autobody parts and chassis parts, crack initiation of burring process and stretched flange is one of the most important problems in sheet metal forming. Although the factor of crack initiation is complicated procedure due to various cutting conditions and inhomogeneous distribution of stress or strain, we could evaluate this phenomenon by developing forming method of the parts, side bending test method and "limit diagram of stretch flange-ability". To prevent from crack initiation of burring process, we also developed original die shape and piercing methods for improving condition of the cutting edge.

1. Introduction

The automotive industry is facing the challenges of reducing body weight in consideration of environmental problems and enhancing crashworthiness, and as a solution for both, use of higher-strength steels for auto bodies is expanding. Use of steels of higher strength, however, poses various technical problems: for instance, poorer steel ductility consequent to higher strength increases the risk of sheet breakage during press forming, which leads to repeated adjustment of dies and increased die manufacturing costs. While high-strength steel sheets having good ductility have been developed in consideration of the problem, approaches from the forming technology side are also of great importance. When high-strength sheets are press formed, special care must be taken since they are more prone than those of conventional strength to cracking from the edge of portions where stretch flanging work is applied. This is because work hardening advances near the edges as a result of strain introduced during blanking, and thus optimizing the conditions of blanking is also of great importance. In consideration of the above, this report presents the method for evaluating material behavior in relation to stretch flanging fracture that causes problems during forming work of high-strength steel sheets, and countermeasures against the fracture.

2. Method for Evaluating Cracking in Stretch Flanging Work

2.1 Test method for evaluating stretch flangeability

Conventionally, the material properties related to stretch flanging work have been evaluated through hole expansion test. Specimens fail in this test wherein strain is substantially evenly distributed in the circumferential direction of the hole. However, in actual manufacturing of automotive parts, strain is often distributed unevenly, as a consequence of which, fracture limit is influenced by strain and stress gradients near the fracture.[1] In addition, since hole expansion test is axisymmetric, the failure occurs in the low-ductility direction, and is therefore different from tensile test, it is difficult to evaluate materials in consideration of anisotropy. Evaluation methods using models of ductile fracture and plastic instability as criteria were proposed [2, 3]; however, the results varied significantly depending on the assumption on the hardness and size of the hardened layer along the hole edge, and attention had to be paid during actual application.

In view of the above, the authors developed a practical test method for evaluating the stretch flanging limit of high-strength steel sheets. Specifically, the method consists of determining the limit of stretch flanging work by forming a specimen sheet into a saddle-like shape defined by straight lines and circular arcs simulat-

* Senior Researcher, Ph.D, Forming Technologies R&D Center, Steel Research Laboratories
20-1 Shintomi, Futtsu, Chiba 293-8511

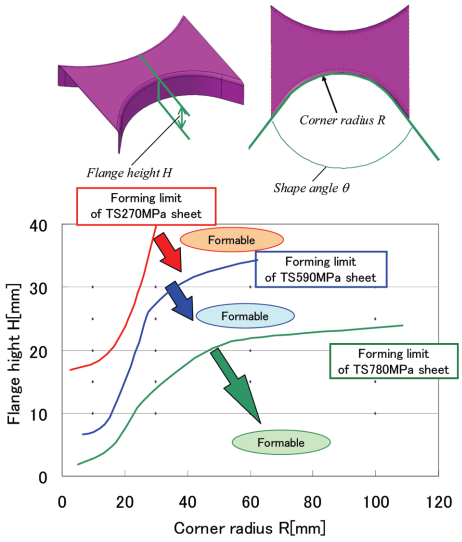

Fig. 1 Stretch flangeability of saddle shape parts and formability map

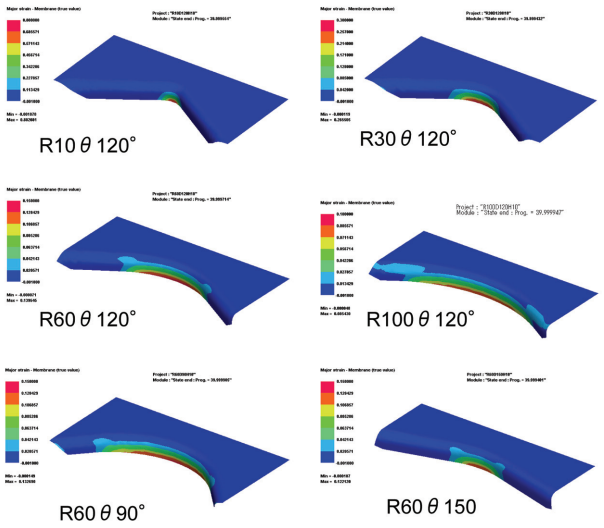

Fig. 2 FEM analysis of major strain distribution (in contours) at stretch flanging into different shapes (flange hight H = 10mm)

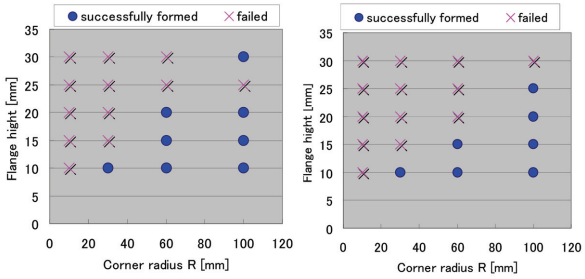

(a) Experimental results (b) FEA results

Fig. 3 Stretch flangeability evaluation map (C/t = 11.0%)

ing the automotive parts formed by stretch flanging.[4] By changing the radius R and the central angle θ of the arc of the saddle-like shape, it is possible to take into consideration the gradients of strain and stress that change depending on the intended shape. **Fig. 1** shows a stretch flangeability evaluation map defining the relationship between the flange height H and corner radius R that can be safely formed using steel sheets of different tensile strengths prepared by blanking; it is possible to confirm the boundary between the feasible and infeasible regions of forming work on the map. The test result data can be effectively used as guidelines in the design of parts to reduce the cost incurred due to defects formed in trial and commercial production.

To evaluate the strain at the time of failure by the developed method, the authors conducted FEM analysis under the same forming conditions. The major strain at the center of the stretched arc flange at the lower dead center was defined as forming strain ε_1. In addition, they conducted hole expanding test according to the Japan Iron & Steel Federation (JISF) standard, converted the thus-obtained hole expansion ratio into logarithmic strain, and defined this logarithmic strain as the critical hole expanding strain ε_{cr}. For the FEM analysis, a specimen was assumed to fail when $\varepsilon_1 \geq \varepsilon_{cr}$ was satisfied.

The FEM analysis showed that strain distribution changed depending on the shape of the stretch flanging portion. **Fig. 2** shows in contours the distribution of major strain obtained through analysis of forming work of pieces having a flange height H of 10 mm. In all the forming shapes, major strain was registered at the edge of the stretch flanging portion, but the width of the region of major strain was different.

As seen in **Fig. 3** (a), in the stretch flangeability evaluation map obtained through tests, the zone of successful forming is larger as the corner radius R increases. Fig. 3 (b) is the stretch flangeability evaluation map obtained through FEM analysis using ε_{cr} as the limit of stretch flanging. When C/t = 11.0% (where C is the die-punch clearance, and t is the sheet thickness), which is close to the condition in industrial practice, the evaluation result is not much different from the test result shown in part (a). This indicates that consideration of the blanking die clearance is essential for predicting the forming limit of stretch flanging and that fracture evaluation based on conventional forming limit diagram (FLD) is inadequate for the purpose.

2.2 Side-bending test

To evaluate stretch flangeability accurately simulating the characteristics of the relevant portion of real parts, the authors studied use of a side-bending test device. While the concept of side-bending tests has long been understood,[5] they developed a new test facility incorporating an image processing system for evaluating the stretch flangeability of high-strength steel sheets.[6] **Fig. 4** shows the outlines of the developed test device, wherein a cylinder head is precisely positioned by a hydraulic servo cylinder to apply an adequate amount of deformation force to a specimen sheet via a jig.

Part (a) of **Fig. 5** shows the geometry of a rectangular sheet test piece 100 mm × 35 mm in size having a semi-circular notch 30 mm in radius, and part (b) schematically illustrates the side-bending action of the jig and the specimen. The shape and conditions of the notch can be changed in consideration of the blank shape for the intended stretch flanging forming. A test piece is clumped at two ends by the jig consisting of two pieces, which are rotated around pivots by the cylinder head to apply tension and rotation to the specimen so as to cause stretch flanging deformation.

A specimen is considered to have failed under stretch flanging when a crack has grown across the sheet thickness, and its limit of stretch flanging is determined based on the strain at the sheet surface. For accurate measurement free of reading errors, a grid is

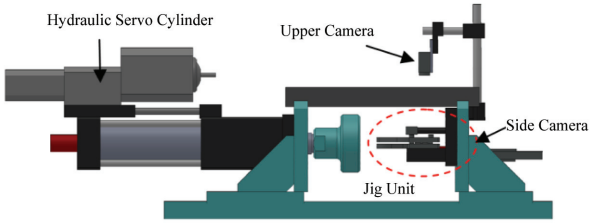

Fig. 4 Schematic view of developed side-bending test device

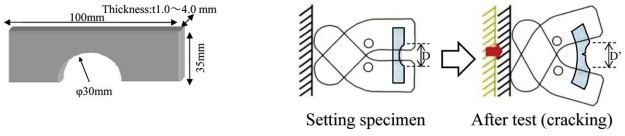

Fig. 5 Schematic view of test piece and method of the side-bending test

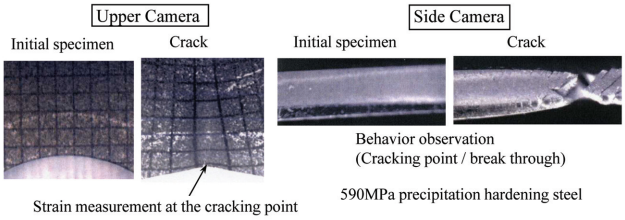

Fig. 6 Identification of strain and observation of crack initiation

drawn on the specimen surface, and the sheet edge of the stretch flanged portion and the sheet surface are observed by two in-line cameras positioned in synchronization with the cylinder head. As an example, **Fig. 6** shows the result of the side-bending test of a 3.2-mm-thick test piece of tensile strength 590 MPa blanked into the geometry given in Fig. 5 (a) at die clearance C/t = 20%. A camera trained at the sheet edge follows it from the initial state to the development of a crack, and the other focusing on the surface in synchronization with the edge camera measures the critical strain when a crack develops across the sheet thickness.

To confirm the accuracy and effectiveness of the side-bending test device, the authors conducted tests using specimen sheets of two steel grades (Materials A and B) 3.2 mm in thickness. The two steels were substantially the same in terms of tensile strength (ca. 590 MPa) and elongation, but different in terms of hole expandability (λ value of Material A was 75% and that of Material B 51%). Test pieces were blanked out from material sheets into the geometry in Fig. 5 (a) at a die clearance of C/t = 20% in three different directions—the rolling direction (L direction), the transverse direction (C direction), and a direction at an angle of 45° (X direction)—and is subjected to side-bending tests. **Fig. 7** shows the results of these test pieces; the circles in the graph indicate the average figure of a lot of 10 test pieces, and the error bars the maximum and minimum readings.

While the limit strain of Material A was substantially the same in the L and C directions, that of Material B in the C direction was lower than that in the L direction, which seems to indicate that the difference between Materials A and B in terms of hole expandability (λ) is due to the difference of their properties in the C direction.

Thus, the side-bending test device proved effective at evaluating

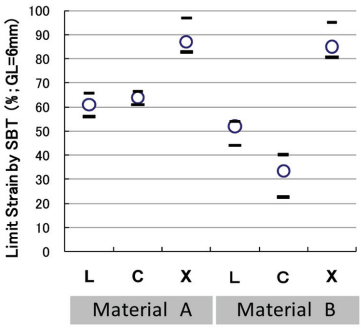

Fig. 7 Difference of the limit strain of two materials

formability in high accuracy and under conditions close to those in actual filed practice. Another advantage of the developed test device is that it allows easy, real-time observations of inside fractures in the flange region and edge fracture, which makes it possible to compare the material characteristics at the edge and in the other portions, making the characteristics required of formed parts clearer. In addition, optimization of material selection and blanking conditions, (tool clearance, shear angle, blanking direction, etc.) before performing actual forming work, is possible by cutting out test pieces from the blank portion to which stretch flanging work is to be applied and subjecting them to side-bending test at a stage of commercial production or machine tuning at start-up production,.

2.3 Limit surface of stretch flangeability

With attention focused on the edge of a blanked sheet, stretch flanging deformation during press forming can be expressed as shown in part (a) of **Fig. 8**. If the strain change along a line from an edge position in the direction away from the edge is considered as strain gradient, the increase in this gradient is considered to suppress the initiation of a crack at the edge position. Also, if the strain change along the edge is considered as the strain concentration, its increase is considered to accelerate the formation of a crack at the peak position. It follows therefore that, since the crack preventing effect of the strain gradient and the crack accelerating effect of the strain concentration compete with each other, the strain at the sheet edge at crack initiation is expected to change depending on the states of these two effects, which makes the fracture behavior under stretch flanging work complicated.

In consideration of the above situation, when fracture strain is viewed to be influenced by the strain gradient and concentration, a three-dimensional limit surface of successful stretch flanging can be defined, as illustrated in part (b) of Fig. 8.[7] The concept of the limit surface makes it possible to take into consideration both the effects of the strain gradient to increase fracture strain and that of the strain

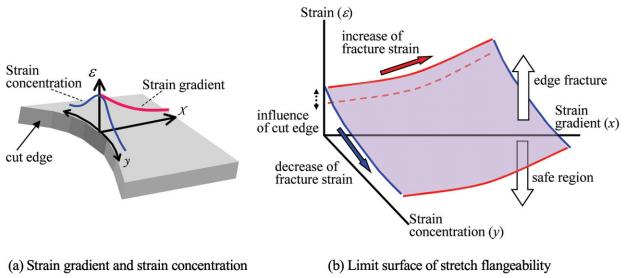

Fig. 8 Effects of strain gradient and concentration and limit surface of stretch flangeability

concentration to decrease it (meaning fracture more likely), and thus to define the amount of strain that leads to fracture in a region where the two are combined with each other; in industrial practice, presumably most stretch flanging work is done in such a region. For this reason, application of the concept of the limit surface to forming test of real parts and forming analysis by FEM is expected to enable prediction of fracture at stretch flanging under varied conditions. In addition, since the formation of a fracture at stretch flanging depends greatly on the condition of sheet edge, the position and shape of the limit surface is likely to change depending on blanking clearance and other factors.

In consideration of the above, using 1.4-mm-thick sheets of three steel types (steels A, B, and C) of a 590-MPa grade as specimens, the authors measured fracture strain under different strain gradients and concentrations. They conducted side-bending tests on specimens of different geometries using the test device described in Sub-section 2.2, as well as a hole expansion test, and a tensile test of blanked edges. Then, on the basis of the fracture strain obtained through combination of the results of these test, they defined the limit surfaces of successful stretch flanging for the three steels. **Fig. 9** shows the limit surfaces; which exhibit characteristic features of their respective steel types. The limit surface of successful stretch flanging of steel A is such that fracture strain decreases as strain concentration increases, and as a result, the steel is likely to fail in wide ranges of stretch flanging work. In contrast, the decrease in the fracture strain of steel B is comparatively less even with a large strain concentration; therefore, steel B is expected to be comparatively resilient even in stretch flanging work into a shape with high deformation concentration such as those having small arc radius *R* in Fig. 2. Because the fracture strain of steel C is large in the region of large strain gradient, steel C is considered to be comparatively resilient in hole expanding and similar working, but likely to fail in the region of large strain concentration.

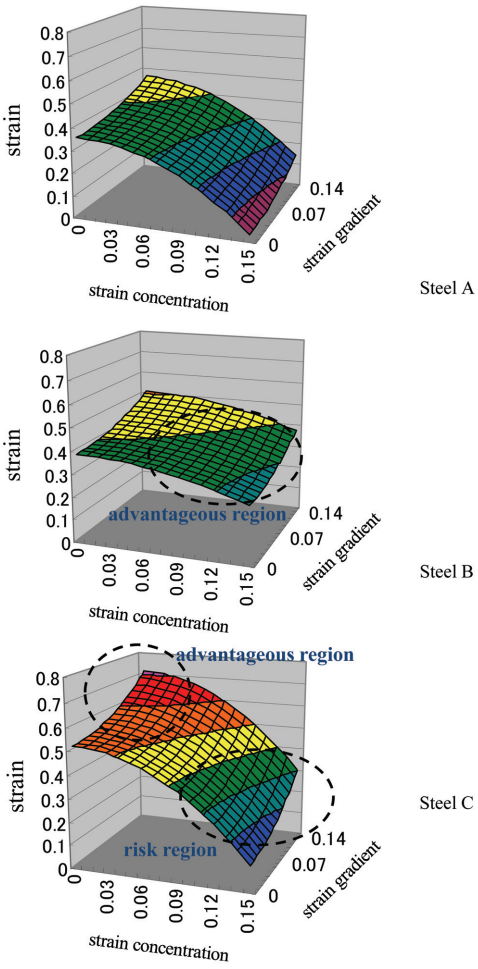

Fig. 9 Limit diagrams of stretch flangeability of different steels

3. Measures to Improve Stretch Flangeability

There have been papers on steel sheet forming technology proposing measures to improve hole expandability by shaving, opposed die shearing, etc.; however, few of those methods are widely practiced owing to cost reasons. Given the situation, two easy-to-use hole punching tools effective at improving hole expandability are presented below: a punch with a hump on the head surface and a die with chamfered edge.

3.1 Improvement of hole expandability by using punch with hump

It has been known that when strain gradient is large, expandability of a punched hole depends on the formation and propagation of a crack at the hole edge, and the smaller the plastic strain introduced at hole punching, the better the hole expandability.[8] This can be inferred from the mechanism of hole expandability based on fracture mechanics.[9] While considering this with an aim toward improving hole expandability, the authors developed a hole punching method whereby the plastic strain of a hole edge is decreased.[10]

Because plastic strain is introduced to a punched edge at the stage of forming a shear surface, it can be decreased by accelerating ductile fracture using the head edge of the punch during blanking work, thus facilitating the formation of cracks. Ductile fracture occurs depending on the stress triaxiality: the larger the triaxiality, ductile fracture results from the smaller equivalent plastic strain.[11] Therefore, by increasing the stress triaxiality of the sheet in contact with the punch-head edge, it is possible to accelerate ductile fracture to reduce the plastic strain introduced to the punched sheet edge. Accordingly, the authors supposed a blanking punch having a hump on the head surface, as shown in **Fig. 10**, so as to apply tension to the steel sheet at the time of shearing to increase stress triaxiality, and evaluated its ductile fracture accelerating effect by FEM analysis.

Fig. 11 compares the mean stress distribution at punching with a humped-head punch and the same with a flat-head punch. The analysis results show that with the humped-head punch, the mean stress near the punch-head edge is larger than that with the flat-head punch. On the basis of this result, the authors conducted hole expansion tests on high-strength hot-rolled steel sheets of tensile strength

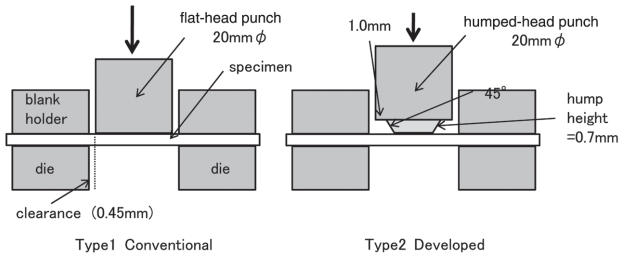

Fig. 10 Schematic diagram of piercing tools used in this study

771 MPa using a punch, as shown in Fig. 10, and calculated limiting hole expansion ratio λ. The test condition was in accordance with the relevant JISF standard [12] except that the initial hole diameter was 20 mm, and the average of limiting hole expansion ratio λ obtained with three test pieces was defined as the value of the specimen.

Fig. 12 shows the limiting hole expansion ratio λ thus obtained; the ratio improved by roughly 20% with the humped-head punch. **Fig. 13** compares the distribution in the rolling direction of the hardness at the edge of holes blanked with the humped- and flat-head punches, and the sectional photographs of Fig. 12 the shapes of the fracture edges. With the humped-head punch, the rate of sheared surface in the fracture surface is lower than with the flat-head punch, and the edge hardness is lower too. From this, the authors confirmed that a hump of a prescribed shape on the head surface of the punch would increase the stress triaxiality in the sheet portion contacting the punch-head edge, thus accelerating the formation of cracks; therefore, it is possible to suppress work hardening of the punched edge and improve hole expandability.

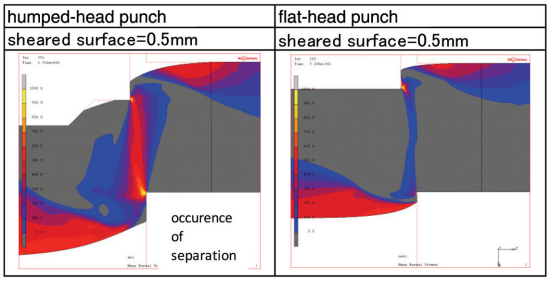

Fig. 11 Calculated distribution of mean stress (σ_m) of cutting process

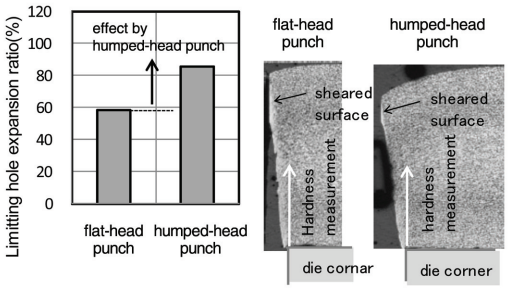

Fig. 12 Effect of limitting hole expansion ratio by humped-head punch

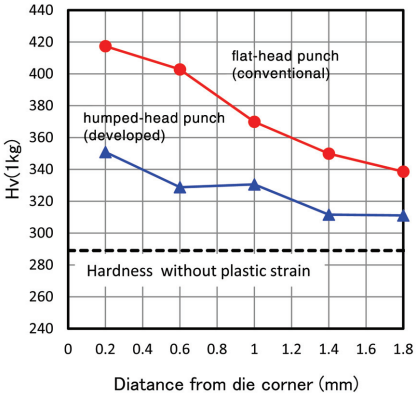

Fig. 13 Hardness distribution near edge after separation

3.2 Improvement of hole expandability by use of punching die with chamfered edge

The hole punching method that uses a die having a large chamfer along the cutting edge [13] is an attempt to simulate hydro-piercing,[14] i.e., a hole punching method using hydraulic pressure as a die, which is known to improve hole expandability; both methods are effective at suppressing shear deformation by the die edge. In this relation, the authors studied the relationship between the dimensions of the die-edge chamfer and hole expandability in the application to high-strength steel sheets, and verified the effects of the method through hole expansion test.

A hole of diameter 10 mm was punched through specimen sheets of dual-phase steel of 590-MPa grade and thickness 1.6 mm, while using dies having edge chamfers, as shown in **Fig. 14**; the value of X was set at 0.0, 1.0, 2.0, 3.0, and 4.0 (X = 0.0 meaning a conventional die without edge chamfer). In addition, the clearance between the punch and die was set at 2.5%, 10%, and 15% of the sheet thickness.

Fig. 15 shows the test results; irrespective of punching die clearance, limiting hole expansion ratio improved significantly for X = 2.0-4.0 from the level of that with a conventional punch without chamfer. The limiting hole expansion ratio with a chamfered punch was roughly 1.5 times that with a conventional punch, an improvement comparable to that by hydro-piercing, shaving, or opposed die shearing.

With regard to the relationship between the chamfer geometry and the limiting hole expansion ratio, Fig. 15 shows that limiting hole expansion ratio either deteriorated or slightly improved when X was 1.0, and it did not improve significantly unless X was 2.0 or more. Further, from the fact that limiting hole expansion ratio did not improve further when X was equal to or larger than a certain value, there is a definite upper limit to the hole expandability obtainable with a chamfered die.

Further, the larger the punching clearance, the smaller the improvement in the limiting hole expansion ratio per unit increase in X.

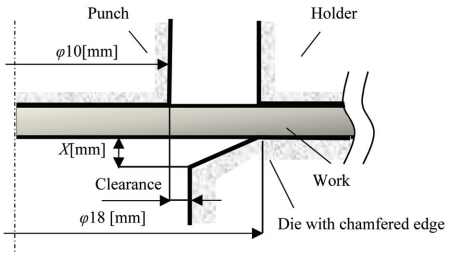

Fig. 14 Schematic view of tool conditions (geometries)

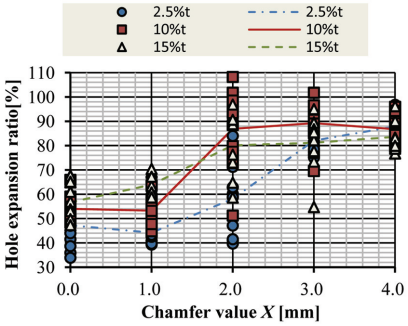

Fig. 15 Effect of hole expansion ratio by chamfered die edge

This is because, with a conventional die without edge chamfer, the larger the clearance, the higher limiting hole expansion ratio. As stated above, there is an upper limit to the improvement of hole expandability, and the value of the hole expandability in the range of X from 3.0 to 4.0 is substantially the same regardless of the clearance. Therefore, with a large clearance, at which the hole expandability with a non-chamfered die was high, the improvement effect of die chamfer was comparatively small.

3.3 Effects of punch shear angle over stretch flangeability

Although many shear blades have an angled edge for improved cutting performance and low noise, there have been few reports on the relationship between the stretch flanging properties of steel sheets and the shear-blade angle. Nevertheless, it may be possible to evaluate stretch flangeability by modifying the method for evaluating it as a continuous value by the side-bending test described in Sub-section 2.2 in such a way that a subtle difference in the setting of a tool such as a change in shear blade angle can be reflected.

Test pieces for the side-bending test were prepared by cutting the semicircular notches with punches of different shear angles, and the relationship between the shear angle and stretch flangeability was investigated.[15] The material of the test pieces was cold-rolled sheets of dual-phase, high-strength steel of a 590-MPa grade, 1.6 mm in thickness, and the geometry of the test pieces was that shown in Fig. 5 (a) in Sub-section 2.2. The semi-circular notches were cut with punches having head faces in five different angles θ from 0.0° to 2.0° measured in the length direction of the test pieces as illustrated in **Fig. 16**, and at clearances of 5%, 10%, and 15% of sheet thickness.

Stretch flangeability was calculated as $(D' - D) / D \times 100$ (%), where D is the initial notch width in Fig. 5 (b), and D' the notch width when a crack at the sheared edge at the center of the notch grew across the sheet thickness at the side-bending test.

Fig. 17 (b) shows that of test pieces prepared at the same blanking clearance, the average hardness in the thickness direction of the portion near the sheared surface was lowest for $\theta = 0.5°$; this shear angle was substantially the same as that with which the ratio of the shear drop at the edge and that of the sheared surface measured separately were smallest. Furthermore, only when $\theta = 0.5°$, the sheet

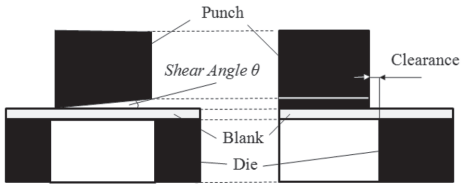

(a) front view (b) side view

Fig. 16 Schematic view of the cutting tool with shear angle

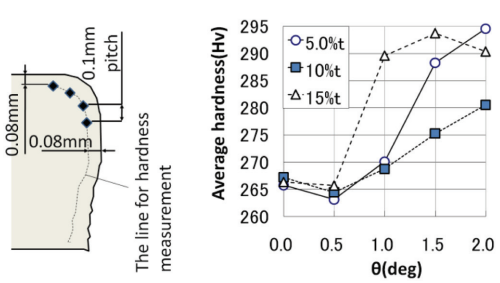

(a) Position of indentation (b) Average hardness of cut edge

Fig. 17 Hardness distribution of the cut edge

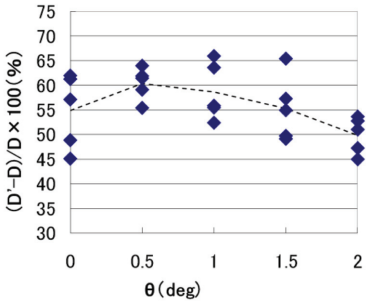

Fig. 18 Effects of shear angle on (over) notch opening at side bending test

hardness was lower than that with a punch without shear angle.

Fig. 18 shows some examples of the side-bending test results. When the blanking clearance was 5.0% of the sheet thickness and the shear angle was 0.5°, the notch width opening was largest. This indicates that there is an optimum shear angle with respect to the notch width opening and at a shear angle larger than the optimum, the stretch flangeability of the sheared edge becomes poorer than that obtained with a punch without shear angle. From comparison of Figs. 17 and 18, it is presumed that the reason why notch opening ratio was better or why its fall was suppressed for $\theta = 0.5°$ than for $\theta = 0.0°$ is that the punch of a shear angle of 0.5° is effective at lowering the work hardening of the material at the center of the semicircular notch.

4. Conclusion

Stretch flangeability is a major property item related to forming work of high-strength steel sheets into automotive parts. This paper has presented methods for its evaluation and measures to improve it in consideration of the mechanisms of stretch flanging. It is expected that combination of these technologies, with the help of FEM analysis, will enable material selection, press forming practice, and process design more suitable for preventing failure in forming work. Development is desired of new technology combining these improved practices with forming machines capable of complicated and delicate control such as servo press forming machines, and optimized forming technology making use of advanced simulation techniques.

References

1) Yoshida, T.: Journal of the Japan Society for Technology of Plasticity (JSTP). 52 (606), 777 (2011)
2) Takuda, H., Ozu, K., Hama, T., Yoshida, T., Nitta, J.: Journal of JSTP. 49 (572), 58 (2008)
3) Itoh, S., Mori, N., Kondoh, T., Uemura, H.: Proc. 56th Japanese Joint Conference for Technology of Plasticity (JJCTP). 2005, p. 45
4) Nitta, J., Yoshida, T., Hashimoto, K., Kuriyama, Y.: Proc. IDDRG 2008. 2008, p. 93
5) Nagai, Y., Nagai, Y.: PK Giho. (6), 14 (1995)
6) Sato, K., Yoshida, T., Mizumura, M., Suehiro, M., Yoshida, H.: Proc. 61st JJCTP. 2010, p. 407
7) Yoshida, H., Miyagi, T., Soto, K., Yoshida, T., Mizumura, M., Suehiro, M.: Proc. 62nd JJCTP. 2011, p. 379
8) Nakagawa, T., Yoshida, S.: RIKEN Report. 44 (3), 150 (1968)
9) Takahashi, Y., Kawano, O., Tanaka, Y., Ohara, M.: Proc. MS&T 2009. Pittsburgh, USA, p. 1317
10) Takahashi, Y., Kawano, O., Horioka, S., Obara, M.: Proc. 62nd JJCTP. 2011, p. 119
11) Hancock, J.W., Mackenzie, A.C.: Journal of the Mechanics and Physics of Solids. 24 (2), 147 (1976)
12) Japan Iron & Steel Federation Standard “Method of hole expanding

test." JFS T 1001, (1996)
13) Matsuno, T., Mizumura, M., Seto, A., Suehiro, M.: Proc. 62nd JJCTP. 2011, p. 123
14) Mizumura, M., Sato, K., Kuriyama, Y.: Proc. 58th JJCTP. 2007, p. 403
15) Matsuno, T., Sato, K., Nitta, J., Seto, A., Mizumura, M., Suehiro, M.: Proc. 61st JJCTP. 2010, p. 409

Hiroshi YOSHIDA
Senior Researcher, Ph.D
Forming Technologies R&D Center
Steel Research Laboratories
20-1 Shintomi, Futtsu, Chiba 293-8511

Tohru YOSHIDA
Chief Researcher, Dr.
Forming Technologies R&D Center
Steel Research Laboratories

Koichi SATO
Senior Researcher, Dr.
Nagoya R&D Lab.

Yuzo TAKAHASHI
Senior Researcher
Oita R&D Lab.

Takashi MATSUNO
Senior Researcher
Forming Technologies R&D Center
Steel Research Laboratories

Jun NITTA
Senior Researcher, Dr.
Forming Technologies R&D Center
Steel Research Laboratories